

A Novel Approach for Measuring Electrical Impedance Tomography for Local Tissue with Artificial Intelligent Algorithm

A. S. Pandya

*Department of Computer Science and Engineering
Florida Atlantic University
Boca Raton, FL 33431, USA*

pandya@fau.edu

A. Arimoto

*Department of Electrical and Electronics Engineering
University of Tokushima
Japan*

arisa922@ee.tokushima-u.ac.jp

Ankur Agarwal

*Department of Computer Science and Engineering
Florida Atlantic University
Boca Raton, FL 33431, USA*

ankur@cse.fau.edu

Y. Kinouchi

*Department of Electrical and Electronics Engineering
University of Tokushima
Japan*

arisa922@ee.tokushima-u.ac.jp

Abstract

This paper proposes a novel approach for measuring Electrical Impedance Tomography (EIT) of a living tissue in a human body. EIT is a non-invasive technique to measure two or three-dimensional impedance for medical diagnosis involving several diseases. To measure the impedance value electrodes are connected to the skin of the patient and an image of the conductivity or permittivity of living tissue is deduced from surface electrodes. The determination of local impedance parameters can be carried out using an equivalent circuit model. However, the estimation of inner tissue impedance distribution using impedance measurements on a global tissue from various directions is an inverse problem. Hence it is necessary to solve the inverse problem of calculating mathematical values for current and potential from conducting surfaces. This paper proposes a novel algorithm that can be successfully used for estimating parameters. The proposed novel hybrid model is a combination of an artificial intelligence based gradient free optimization technique and numerical integration. This ameliorates the achievement of spatial resolution of equivalent circuit model to the closest accuracy. We address the issue of initial parameter estimation and spatial resolution accuracy of an electrode structure by using an arrangement called “divided electrode” for measurement of bio-impedance in a cross section of a local tissue.

Keywords: Artificial Intelligence, Alopex Algorithm, Divided Electrode Method, Electrical Impedance Tomography, Equivalent Circuit Model, Medical Imaging

1. INTRODUCTION

Biological tissues have complex electrical impedance related to the tissue dimension, the internal structure and the arrangement of the constituent cells. Therefore, the electrical impedance can provide useful information based on heterogeneous tissue structures, physiological states and functions [1, 2]. In addition the concepts of time varying distribution of electrical properties inside a human body such as electrical conductivity and (or) permittivity can be used to analyze a variety of medical conditions. High-conductivity materials allow the passage of both direct and alternating currents and high-permittivity materials allow the passage of only alternating currents. Both of these properties are of interest in medical systems since different tissues have different conductivities and permittivities [3, 4].

In an effort to obtain more precise evaluations of tissues for diagnostic purposes, bio-impedance measurements can be focused on specific local tissues such as tumors, mammary glands and subcutaneous tissues [5]. Most importantly tissue impedance at zero frequency, corresponding to extra cellular resistances is particularly useful for evaluating mammary glands, lung cancers and fatty tissues [6, 7, 8]. In comparison with x-ray images, ultrasonic images and magnetic resonance imaging (MRI), electrical impedance measurement is inexpensive.

A variety of medical systems such as X-ray, CT, MRI and Ultrasonic Imaging are used for medical tissue diagnosis. These systems create a two-dimensional (2D) image from the information based on density distribution of the living tissue. On the other hand, EIT (also called Applied Potential Tomography) creates a two-dimensional image from information based on the impedance characteristics of the living tissue. This information acquired through EIT can be clinically very useful. For example, in order to obtain precise evaluations of tissues for diagnostic purposes, bio-impedance measurements can be focused on the specific local tissues such as tumors, mammary glands and subcutaneous tissues [5]. Additionally, EIT could be extremely convenient in several medical conditions requiring bedside therapies such as Pulmonary Oedema, Cerebral Haemorrhage and Gastric Emptying among others. Typically, conducting electrodes are attached to the skin of the subject and small alternating currents are applied to some or all the electrodes in a traverse plane. These are linked to a data acquisition unit, which outputs data to a computer. By applying a series of small currents to the body, a set of potential difference measurements can be recorded from non-current carrying pairs of electrodes.

When it comes to practical implementation of EIT, there are several limitations such as the complicated spatial distribution of the bio-impedance that arises from complex structure of biological tissues, in addition to the structure and arrangement of measurement electrodes. To obtain reasonable images, at least one hundred, and preferably several thousand, measurements are usually carried out. This results in relatively long time for measuring and analyzing specifically, due to changing combination of pair of electrodes. Therefore, in many instances, it is difficult to achieve high precision and to assert measurement results as clinically relevant information.

In order to overcome this drawback, there is a need to address several issues for employing EIT in medical application such as, estimating impedance parameters for local tissue (i.e. inner tissue impedance distribution) and the shape of electrode structure. In this paper, we address the issue of electrode structure by using an arrangement called "Divided Electrode" for measurement of bio-impedance in a cross section of a local tissue. The determination of local impedance parameters can be carried out using an equivalent circuit model. However, the estimation of inner tissue impedance distribution using impedance measurements on a global tissue from various directions is an inverse problem. Hence it is necessary to solve the inverse problem of calculating

mathematical values for current and potential from conducting surfaces. Experiments were then conducted by using two different algorithms, Newton Method and Alopex method for determination of impedance parameters in the equivalent circuit model. Newton method is deterministic since it uses steepest descent approach while Alopex is a stochastic paradigm.

Experimental results show that, higher accuracy can be obtained while estimating the parameter values with Newton method. However, selecting an appropriate set of initial parameters with Newton method is highly complicated and is based on trial and error. This translates into a leading disadvantage in the effectiveness of Newton method. Since Alopex is a stochastic approach it is able to seek out the global minima using any arbitrary set of parameter values. However it takes several iterations and often converges on a near optimum solution rather than the precise parameter values. Therefore, to obtain results with appropriate initial parameters with high accuracy, simulations were carried out using a novel approach, which relies on stochastic approach initially and then uses deterministic calculations to obtain the final parameter values with a high accuracy. Thus, the novel method overcomes the distinct disadvantage of each of the methods. Overall this ameliorates the performance of spatial resolution of equivalent circuit model to the closest accuracy.

2. BACKGROUND

EIT system primarily comprises of the electrodes attached to a human body, a data acquisition unit and an image reconstruction system. Voltage is measured through data acquisition system, which is then passed to another system for reconstruction the image [9]. The goal here is to distinguish various tissue types. This is possible because the electrical resistivity of different body tissues varies widely from 0.65 ohm-m from cerebrospinal fluid to 150 ohm-m for bone. T. Morimoto and Uyama, while studying the EIT for diagnosis of pulmonary mass emphasized that the electrical properties of biologic tissues differ depending upon their structural characteristics and differences in the electrical properties of various neoplasms [10]. As impedance is an important electrical property, intra operative impedance analysis can be used to measure the impedance of pulmonary masses, pulmonary tissues, and skeletal muscle [5].

The first impedance imaging system was the impedance camera constructed by Henderson and Webster [11]. This system used a rectangular array of 100 electrodes placed on the chest that were driven sequentially with a 100 kHz voltage signal. A simple conductivity contour map was produced based on the assumption that current flows in straight lines through the subject. This was one of the initial efforts towards practical implementation of EIT technology in a medical system. In [47], Agarwal et al. have discussed the novel approach medical image reorganization with GMDH algorithm.

In the early eighties, Barber and Brown constructed a relatively simple yet elegant EIT system using 16 electrodes by applying the constant amplitude current at 50 kHz between two electrodes at a time [12]. Ten images per second were generated, which were computed using back-projection. This method has been applied with great success in the field of X-ray tomography. The image depicted the structure of bones, muscle tissue, and blood vessels. However, the resolution of the image was very low. This image is generally regarded as the first successful vivo image generated by an EIT system.

There are mainly two methods in EIT that have been explored in depth: 2-D EIT and 3-D EIT. Commonly, 2D EIT systems could be divided into two different category sets namely: Applied Potential Tomography (APT) and Adaptive Current Tomography (ACT). In 2-D EIT system electrodes are positioned at an equal spacing around the body to be imaged thus, defining a plane through the object. Images are then reconstructed assuming that the data were from a 2-D object. These objects mainly demonstrate a significant amount of contribution to the image from off-plane conductivity changes. It further implies that unlike in any 3D X-ray image that can be constructed from a set of independent 2-D images, for 3D EIT it is necessary to reconstruct

images from data collected over the entire surface of the object volume [13]. Metherall, et al, 1996, researched the impact of off-plane conductivity changes on to the reconstructed image in 2-D EIT. Metherall et al, [14] further studied 2D EIT and used these observations to further carry out comparisons between 2D and 3D EIT. They produced the images using a 16-electrode system with interleaved drive and receive electrodes [15]. With the 3-D methods, the reconstructed images are more accurate as compared to original images. Lionheart et al [16] constructed a 3D EIT image at Oxford Brookes University. They constructed a time average EIT image of cross section of a human chest. For constructing a 3-dimensional (3D) EIT image, conducting electrodes were attached around the chest of a patient. The lungs were presented as a low conductivity region. The resulting image was a distorted image as a 2D reconstruction algorithm was employed instead of a 3D reconstruction algorithm [17].

2.1 Challenges in EIT

There are few issues that need to be addressed for implementing EIT in practical medical systems: (1) the complicated spatial distribution of the bio-impedance that arises from obscure structure of biological tissue; (2) the structure and arrangement of measurement electrodes.

In EIT realm for local tissue a new simulation method was introduced which is a combination of divided electrodes and guard electrodes [18]. In this method required data are obtained by one time measurement. In this paper, we evaluate the efficiency of the new method by computer simulations, where a typical multilayer tissue model composed of skin, fat, and muscle is used. As an example, conductivity distribution in a cross section of the local tissue is estimated using the resistances measured by the divided electrodes. Tissue structures are also estimated simultaneously by increasing the number of the divided electrodes.

Estimation of inner tissue impedance distribution using impedance measurements on a global tissue from various directions is an inverse problem. This results in relatively long time for measuring and analyzing especially due to changing combination of pair of electrodes. There are various concerns that need to be addressed for implementing and deploying EIT system in a real world scenario as a medical imaging system. This includes estimating parameters and electrode structure. Therefore, in many instances, it is difficult to achieve high precision and exactly define the measurement result as clinically relevant information.

2.2 EIT Applications

In EIT imaging, significant alterations in interior properties could result only in minor changes in the measurements [19], implying that it is nonlinear and is extremely ill posed in its behavior resulting the need for high-resolution image measurements with very high accuracy. Thus, converting EIT principles into a commercial application is a challenging process.

There are two main methodologies that have addressed this issue: Applied Potential Tomography (APT) system and Adaptive Current Tomography (ACT) system. APT was developed by Barber and Brown in Sheffield, England [20]. APT system has been successfully employed in the research of various physiological processes, such as blood flow in the thorax, head, and arm, pulmonary ventilation and gastric emptying. ACT was developed at Rensselaer Polytechnic Institute. ACT method has been employed to produce images of the electrical conductivity and permittivity in the human thorax, and breast studies. EIT techniques can be applied to a medical system for acquiring constructive information. This results in various applications [21].

Breast Imaging Using EIT [22, 23]: In [46] Ahmed et al. have provided a detailed review about breast cancer prognosis. X-ray mammography is the standard imaging method used for early detection of breast cancer. However, this procedure is extremely uncomfortable and painful for most women. The high cost of the system forbids its widespread use in developing countries. In addition, the ionizing radiation exposure is damaging to the breast tissue and its harmful effects

are cumulative. This method further suffers from high percentages of missed detection and false alarms resulting in fatalities and unnecessary mastectomies.

On the other hand, EIT is an attractive alternative modality for breast imaging. The procedure is comfortable; the clinical system cost is a small fraction of the cost of an X-ray system, making it affordable for widespread screening. The procedure further poses no safety hazards and has a high potential for detecting very small tumors in early stages of development [24]. Hartov et al. at Dartmouth constructed and analyzed a 32-channel, multi-frequency 2D EIT systems. Newton's method was the base for the image construction [25]. Osterman et al. further modified the Dartmouth EIT system in a way, so as to make it feasible for routine breast examinations [26]. More efforts were later put in, in order to achieve more consistency of the results with an improved breast interface [24].

EIT in Gastrointestinal Tract: EIT images of the lungs and gastrointestinal system were published in 1985 [27]. Studies were undertaken to assess the accuracy of the gastric function images and good correlation with other methods was obtained. Experiments were also undertaken to assess the system's use for monitoring respiration, cardiac functions [28], hyperthermia [29], and intra-ventricular haemorrhage in low-birth weight neonates. This study established that, citrate phosphate buffers can be used as an alternative test liquid for EIT monitoring, and that pH has a systematic effect on gastric emptying and the lag phase [30].

Hyperthermia: In 1987 in vitro and in vivo studies were carried out to determine the feasibility of imaging local temperature changes using EIT to monitor hyperthermia therapy [31]. EIT may be used for temperature monitoring because tissue conductivity is known to change with temperature. Malignant tumors might be treated by artificially increasing temperature by microwave radiation or lasers.

3. EQUIVALENT CIRCUIT MODEL

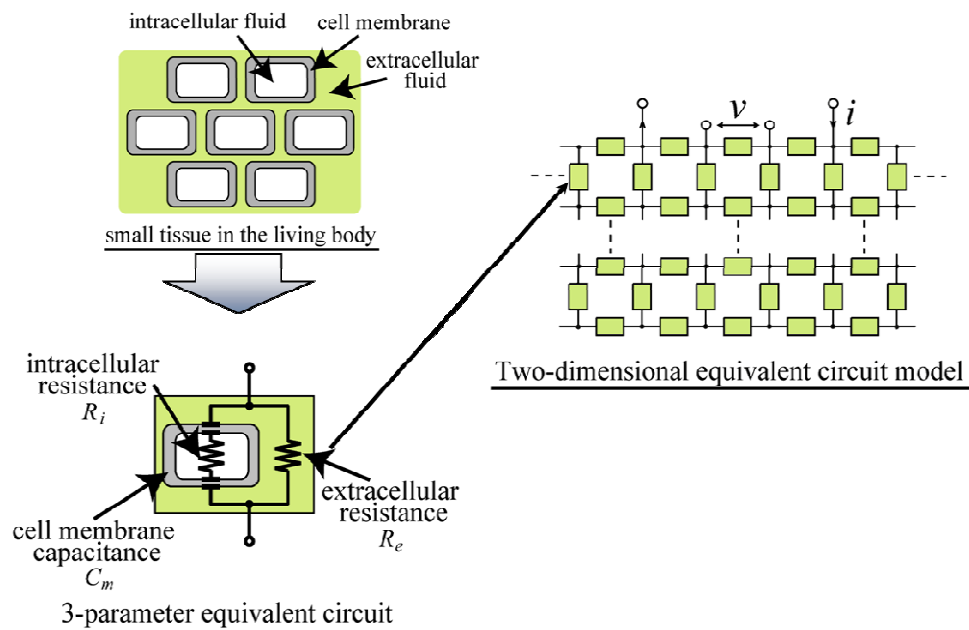


Figure 1: Equivalent Circuit Model.

In every living tissue there is always spatial non-uniformity present even if it is the same tissue such as muscular or hepatic tissue. The presence of this non-uniformity within the living tissue can be determined by using either the Cole-Cole distribution [32] or the Davidson-Cole

distribution [33] to estimate the distribution of the time constant (electric relaxation time) of the circuit model. In this research, impedance distribution in the tissue cross section is represented by a 2D distributed equivalent circuit model as shown in Figure 1.

This spatial distributed equivalent circuit is used to model at individual cell or small tissue level. Therefore, it reflects the impedance spatial distribution. In other words, each small tissue is expressed as an equivalent circuit, which can be expressed using three parameters, namely, the intracellular and extracellular resistances denoted as R_i and R_e respectively, and cell membrane capacitance denoted as C_m . In this model, equivalent circuits with three parameters are connected in the shape of a lattice. The electrodes used to measure v and i are assumed to be point electrodes.

4. DIVIDED ELECTRODE METHOD

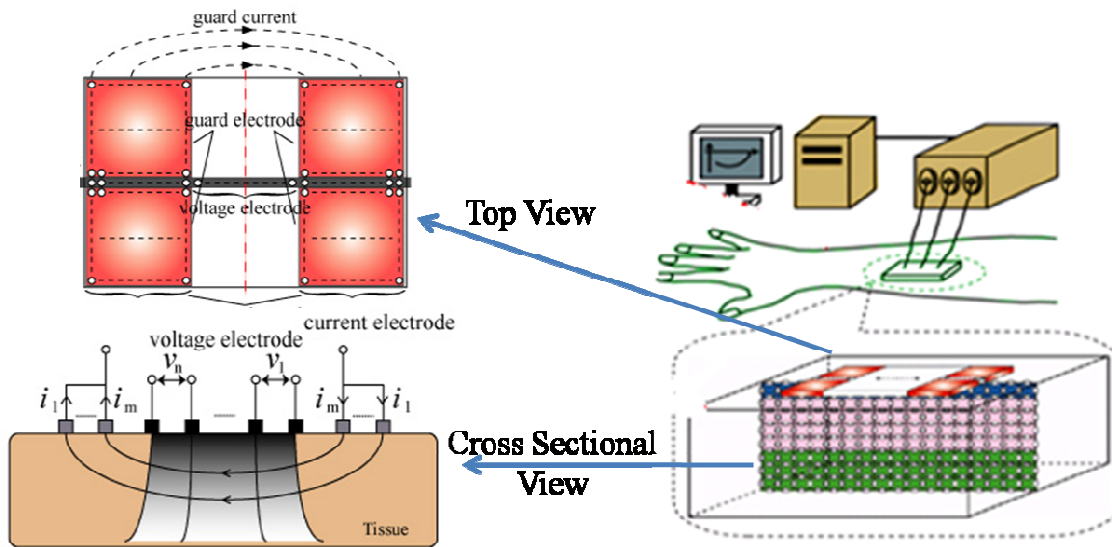


FIGURE 2: Experimental setup for Divided Electrode Method for Impedance Measurement.

The divided electrode method for impedance measurement, which was used in this study, is shown in Figure 2. The figure also shows the top view and the cross sectional view of the divided electrode arrangement. This type of electrode is referred to as divided electrode because it has a shape of a plate, which is divided by slits.

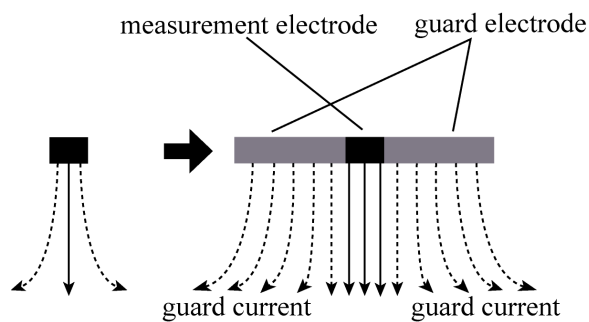


FIGURE 3: Placement of Guard Electrodes on Both Sides of the Current Electrode.

Note that the current electrodes are arranged on both sides of the voltage electrode, which is located in the centre. The current flows simultaneously from all the current electrodes. To control the flow of the current, a guard electrode is placed around each current electrode. Figure 3 shows this arrangement.

Due to the presence of this guard electrode the current from the current electrode flows right into the cross section without spreading. This allows us to measure the value of the 2D impedance distribution [34, 35]. The current electrodes control the measuring range in the direction of depth while the voltage electrodes are employed for controlling the measuring range in the direction of the electrode-axis. Therefore, the number of impedance values obtained at once is given by $\{m \times n\}$ where m is the number of current electrodes (i_1, i_2, \dots, i_m) and n is the number of voltage electrodes (v_1, v_2, \dots, v_n). This allows one to obtain high-resolution measurements at a high-speed.

5. ESTIMATION METHOD

Figure 4 shows the system model for the proposed novel approach. As shown in the Figure 4, the proposed noble approach, we use the Alopex algorithm – a stochastic approach, to determine the initial set of parameter values. Later, deterministic calculation (Newton’s method) is applied to calculate the final set of parameters with high accuracy and precision.

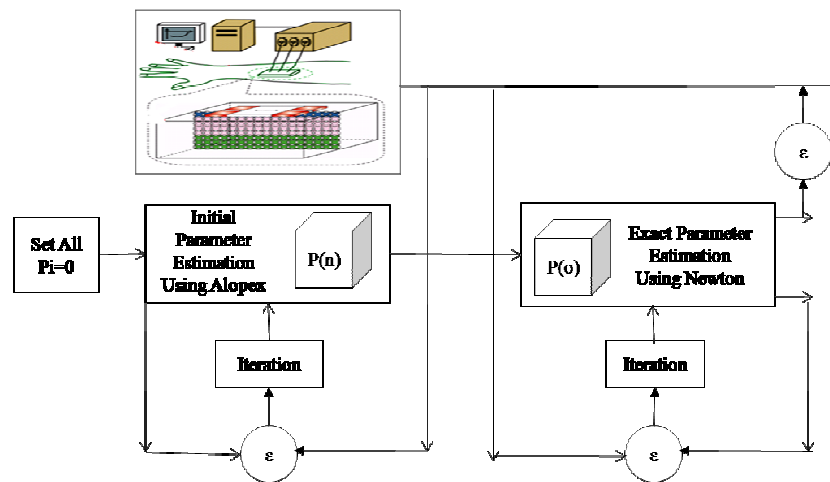


Figure 4: System Model for the Proposed Novel Approach.

5.1 Alopex Algorithm

Alopex (Algorithm for Pattern Extraction) is an iterative process [36], which was originally proposed for the study of visual receptive fields of frogs, relied on optimization based on cross-correlations rather than derivatives. Originally the goal of Alopex was to find a visual pattern (an array of light intensities) which maximizes the response from individual neurons in the brain [37, 36, 38]. Later the Alopex algorithm was developed [38, 39] for application to a variety of optimization problems where the relationship between the cost and optimization parameters cannot be mathematically formulated. In 1990 Pandya [39, 40, 41] introduced Alopex as a learning paradigm for multi-layer networks. They claimed their new version of Alopex to be network-architecture independent, which does not require error or transfer functions to be differentiable and has a high potential for parallelism [42]. Since then, many versions of the ALOPEX have been developed [43, 44, 45].

As a generic optimization framework, ALOPEX has certain prominent advantages. It is a gradient free optimization method, totally network architecture independent and provides synchronous learning. These exclusive features make ALOPEX a distinguishable tool for optimization and

many machine learning problems [42]. In optimization process, Alopex chooses set of variables, which actually describe the state of the system at any given time. A “cost function” F is derived as a function of these variables. The cost function now acts as a object of the optimization process and represents the degree of the closeness of the system to several possible states, one of which is the desired, in our context it is the ‘error minimization’. At each iteration, the values of these variables get updated and cost function is recalculated. Over several iterations the cost function can be brought to an absolute minimum. This state is referred as “convergence” or “global minimum”. Similarly Artificial Neural Networks have found several applications in medical field [48].

5.2 Mathematical Framework for Novel Approach

In order to evolve a model connecting N equivalent circuits with three parameters as shown in Figure 1 it is necessary to estimate the circuit parameter p. Here p is a vector composed of circuit parameters, Ri, Re and Cm corresponding to N circuits. This is an inverse problem and the p values must be estimated using measured impedance data. Impedance data ZD measured by K electrodes arrangement is expressed as:

$$Z_p(\omega) = [Z_p^{(1)}(\omega), Z_p^{(2)}(\omega), \dots, Z_p^{(K)}(\omega)]^T \tag{1}$$

The parameter vector p is expressed as:

$$p = [R_e(1), R_i(1), C_m(1), \dots, R_e(N), R_i(N), C_m(N)]^T \tag{2}$$

The initial value of the parameter p is set to p0. The proposed novel method relies on a stochastic approach during the initial period of estimation and then uses deterministic calculations to obtain the final parameter values with a high accuracy. During the initial stochastic phase the value of the error is calculated using equation 3:

$$\varepsilon = \sqrt{\frac{1}{M} \frac{1}{K} \sum_{i=1}^M \sum_{j=1}^K \left| \frac{Z^{(j)}(p_e, \omega_i) - Z_p^{(j)}(\omega_i)}{Z_p^{(j)}(\omega_i)} \right|^2} \tag{3}$$

Where, M, N, K, ZD and ωi denote the number of voltage electrodes, number of current electrodes, number of frequencies, impedance values calculated using the equivalent circuit model, and the value of the frequency respectively. During the initial phase, at the nth iteration the Pi(n) value is calculated as follows:

$$\delta Pi(n) = Pi(n - 1) + \delta Pi \tag{4}$$

where δPi is given by:

$$\begin{aligned} \Delta i(n) &= +d \text{ with probability } P \\ &= -d \text{ with probability } 1 - P(\Delta_i(n)) \end{aligned} \tag{5}$$

$$\Delta_i(n) = \{p_i(n - 1) - p_i(n - 2)\} \{\varepsilon(n - 2) - \varepsilon(n - 1)\} \tag{6}$$

Where is given by,
and the value for P(Δi(n)) is given by:

$$P(\Delta_i(p)) = \left(\frac{1}{1 - e^{-\frac{\Delta_i(p)}{T}}} \right) \tag{7}$$

In equation 7, T represents the temperature value. Using the p(n) values the corresponding Z(p,ω) value is calculated based on the equivalent circuit model and equation 3 is used to determine the error. Once the value of the error is within the tolerance limit the estimation of p values is switched to a deterministic algorithm. The goal here is to change the value of Z, by changing the value of p so that δZ approaches to zero.

$$\delta Z(p, \omega) = Z_p(\omega) - Z(p, \omega) \tag{8}$$

The mathematical equations for calculating the final value of the error and the estimated parameters are calculated using the following equations:

$$\delta Z(p, \omega) = \left[\frac{\delta Z(p, \omega)}{\delta p} \right]_{p_0} \delta p \tag{9}$$

$$b = A \delta p \tag{10}$$

Where the value of A is:

$$A = \left[\left[\frac{\delta Z(p, \omega_1)}{\delta p} \right]_{p_0}, \dots, \left[\frac{\delta Z(p, \omega_N)}{\delta p} \right]_{p_0} \right]^T \tag{11}$$

Here A is an M×N x K matrix and b is a K-dimensional vector. Substituting the value of A from equation 11 in equation 10, the equation 10 becomes,

$$b = [\delta Z(p, \omega_1)^T, \dots, \delta Z(p, \omega_N)^T]^T \tag{12}$$

Z(p,ω) can be obtained using the p values and the equivalent circuit model. Here, A can be obtained from the numerical analysis based on the equivalent circuit model shown in Figure 1. Therefore, calculation of the least squares method of equation 11 is expressed by equation 12 to obtain δp, which denotes the change in the parameter value with respect to the initial value p0.

6. SIMULATION RESULTS

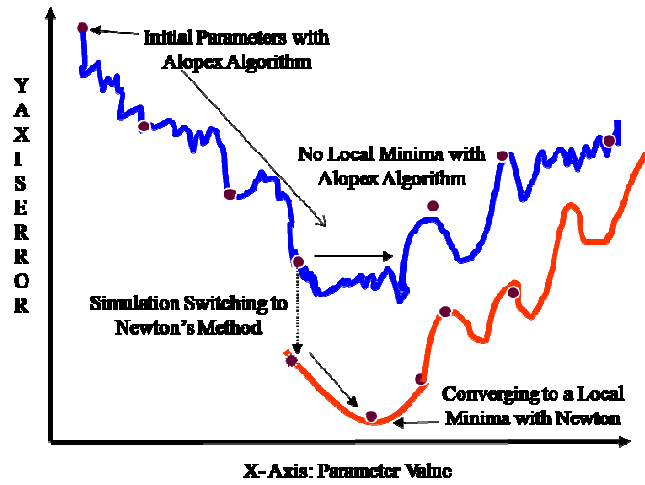


FIGURE 5: Convergence Graph for the Proposed Noble Algorithm.

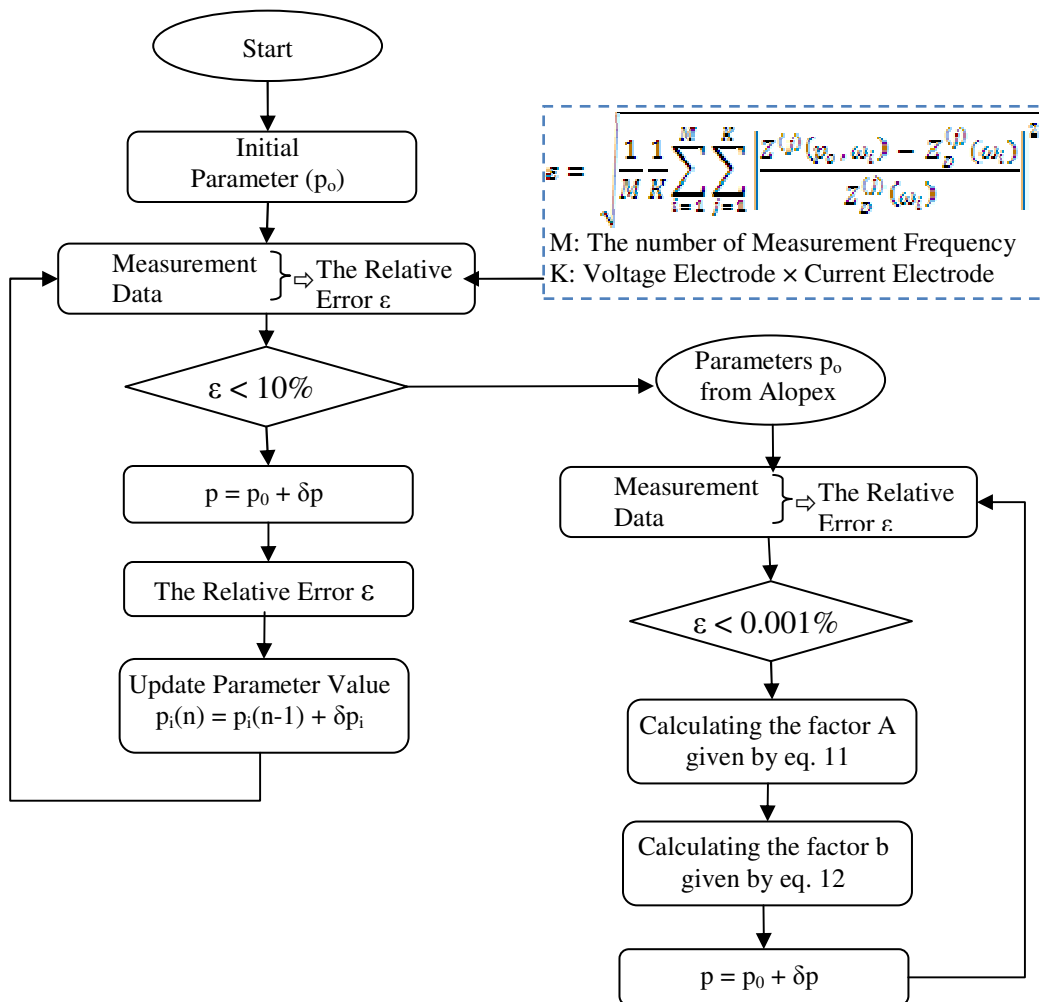
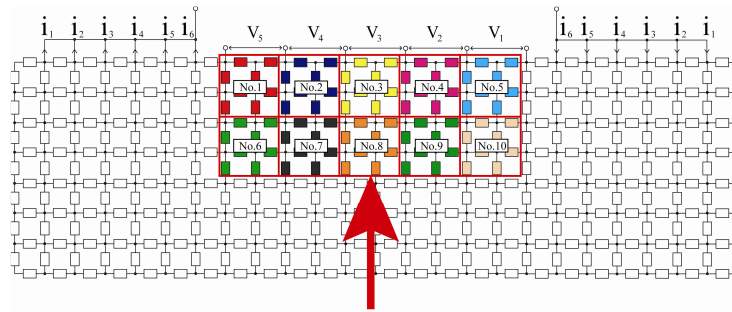


FIGURE 6: Algorithm for the Proposed Novel Approach.

Ideally, a deterministic method like Newton Method yields quick convergence for inverse problems. However, in this case it was found that Newton method often failed to converge due to the presence of local minima, if the initial parameter set was not reasonably close to the global minimum. Selecting a set of appropriate initial parameters with Newton's method is highly complicated and is based on trial and error. Alopex being a stochastic method takes several iterations (in the order of thousands) to converge. However, it is able to seek out the global minima from any arbitrary set of initial parameters.

Figure 5 shows that the proposed novel approach employs Alopex algorithm for selecting the initial parameter value. Once the error value converges within the acceptable bound, the Newton's method is employed for converging to local minimum. Figure 6 shows a flow chart for the final algorithm for the proposed novel approach.



Range of investigation of spatial resolution
FIGURE 7: The Tissue Divided into 10 Parts.

Figure 7 shows the equivalent circuit model used for our simulations, where a tissue is divided in to 10 cells. Since each cell (or equivalent circuit) has 3 parameters, this model involves 30 parameters. The number of voltage electrodes is 5 (M) and the number of current electrodes is 6 (N). The number of measurement frequencies is 10 (K) in the range of 0 to 100[kHz] (ω). Therefore, the number of measurement data is $5 \times 6 \times 10 = 300$.

Table 1 shows the model parameters and the initial estimated parameter for the proposed novel algorithm. Alopex algorithm converges to initial parameter values such that the error is within the 10% range. The final values obtained from the Alopex algorithm are represented as the estimated parameter values in Table 1.

Parameter Values		Re[Ω]	Ri[Ω]	Cm[nF]
Model Parameters	No. 1	180	180	10
	No. 2	80	70	11
Initial Parameters	No. 1	0	0	0
	No. 2	0	0	0
Estimated Parameters	No. 1	174.9	161.8	6.9
	No. 2	86.0	117.7	17.6

TABLE 1: Selecting Initial Parameters through Alopex Method.

Note that here model parameter values represent the global minimum for parameter values for p. No.1 relates to the 2-D model while no.2 relates to the 3-D model. These values were obtained by actually removing the living tissue through dissection and measuring the values. The initial parameter values were set to 0 for Alopex for both models.

The estimated parameter values from Table 1 are applied as the initial parameter values for determining the final values of all the parameters as shown in Figure 6. One can clearly analyze that the output (estimated parameter) from Table 1 is the input (initial parameters) in Table 2.

Parameter Values		Re[Ω]	Ri[Ω]	Cm[nF]
Model Parameters	No. 1	180	180	10
	No. 2	80	70	11
Initial Parameters	No. 1	174.9	161.8	6.9
	No. 2	86.0	117.7	17.6
Estimated Parameters	No. 1	180.0	180.0	10.0
	No. 2	80.0	70.0	11.0

TABLE 2: Calculating the Final Values through Newton's Method.

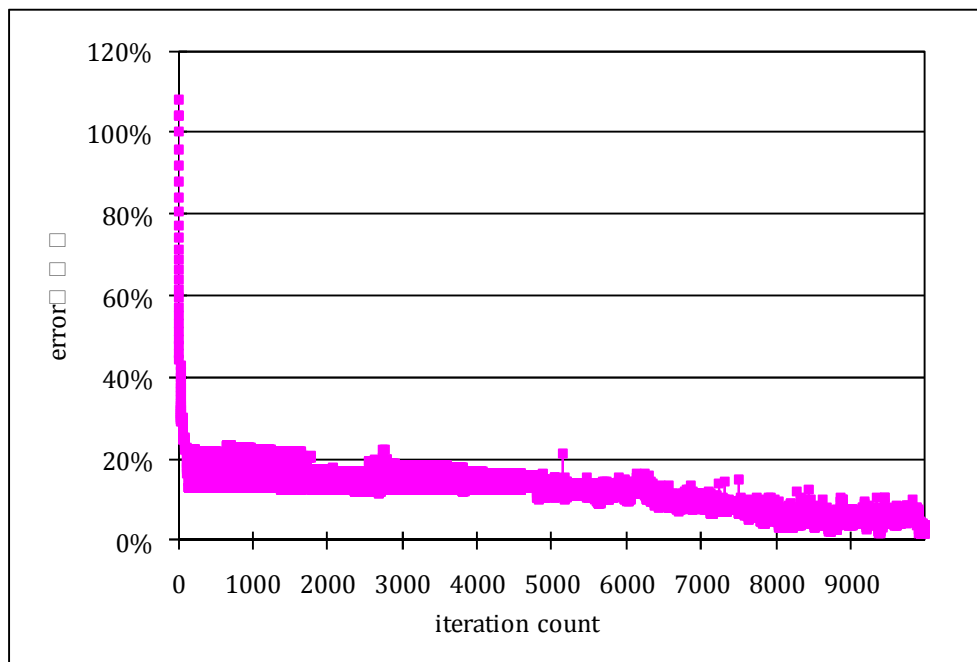


FIGURE 8: Convergence Graph Using the Alopex Algorithm.

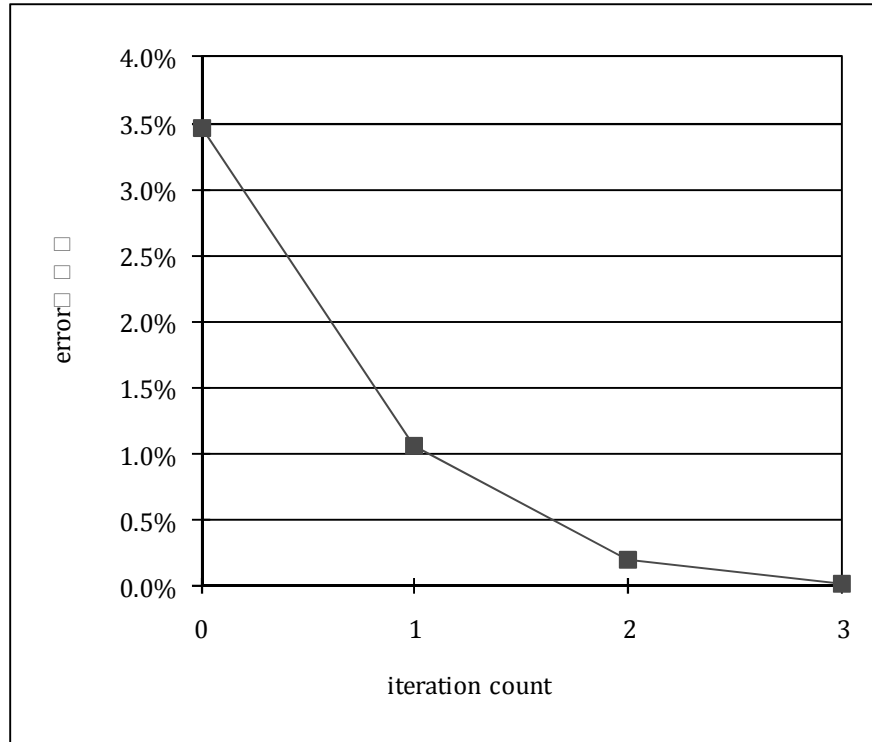


FIGURE 9: Convergence Graph Using the Proposed Novel Algorithm.

Figure 8 shows the error value as a function of iterations during the stochastic phase. Figure 9 shows the error values starting at 3.5% (ending value in Figure 8) and converging to zero within 3 iterations during the deterministic phase.

7. CONCLUSION

EIT, a non-invasive method, creates a two-dimensional image from information based on the impedance characteristics of the living tissue. In this paper a living tissue is represented by the two-dimensional equivalent circuit. The equivalent circuit is composed of intracellular and extracellular resistances R_i , R_e , and cell membrane capacitance C_m which allows for modelling the non-uniformity of living tissue. The paper addresses the issue of electrode structure by using an arrangement called “divided electrode” for measurement of bio-impedance in a cross section of a local tissue. Its capability was examined by computer simulations, where a distributed equivalent circuit was utilized as a model for the cross section tissue. Further, a novel artificial intelligence based hybrid model was proposed. The proposed model ameliorates the achievement of spatial resolution of equivalent circuit model to the closest accuracy. While measuring the impedance value, it is extremely important to estimate appropriate values for all initial parameters. However, estimation of these initial parameters using Newton’s method is extremely difficult. The proposed novel algorithm which uses a combination of stochastic and deterministic approach addresses this issue. Thus, the results obtained were highly accurate.

8. REFERENCES

1. Walker D. C. Et al, “Modelling electrical impedivity of normal and premalignant cervical tissue”, *Electronic Letters*, 36(19):1603-1604, 2000

2. Walker D. C. Et al, "*Modelled current distribution in cervical squamous tissue*", *Physiological Measurement*, 23(1): 159-168, 2002
3. M. Cheney and D. Isaacson, "*Distinguishability in impedance imaging*", *IEEE Transactions on Biomedical Engineering*, 39: 852–860, 1992.
4. M. Cheney, D. Isaacson, and J. C. Newell, "*Electrical impedance tomography*", *SIAM Review*, 41(1): 85–101, 1999.
5. S Kimura, T Morimoto, T Uyama, Y Monden, Y Kinouchi and T Iritani, "*Application of electrical impedance analysis for diagnosis of a pulmonary mass*", *Chest Journal*, 105: 1679-1682, 1995
6. Y. Kinouchi, T. Iritani, T. Morimoto et al, "*Fast in vivo measurement of local tissue impedance using needle electrode*", *Medical and Biological Engineering and Computing*, 35: 486-492, 1997
7. Xueli Zhao, Y. Kinouchi, E. Yasuno, "*A new method for non invasive measurement of multilayer tissue conductivity and structure using divided electrode*", *IEEE Transaction on Biomedical Engineering*, 51(2): 362-370, 2004
8. H. Kato, E. Yasuno, Y. Kinouchi, "*Electrical impedance tomography for local biological tissue*", *Proceeding of 8th International Conference on Control Robotics, Automation and Vision*, 942-946, 2004
9. V. Cherepenin, A. Karpov, A. Korjnevsky, V. Kornienko, Y. Kultiasov, M. Ochapkin, O. Trochanova and D. Meister, "*Three-dimensional EIT imaging of breast tissues: system design and clinical testing*", *IEEE Transaction Medical Imaging*, 21(6): 662-667, 2002
10. T. Morimoto, Y. Kinouchi, T. Iritani, S. Kimura, Y. Konishi, N. Mitsuyama, "*Measurement of the electrical bio-impedance of breast tumors*", *Journal of European Surgical Research*, 102: 86-92, 1990
11. R. P. Henderson, J. G. Webster, "*An impedance camera for spatially specific measurements of the thorax*", *IEEE Transaction on Biomed. Engineering*, 25: 250-254, 1978
12. T. Tang, S. U. Zhang, R. J. Sadleir, "*A portable 8-electrode EIT measurement system*", *IFMBE Proceeding*, 3980-3983, 2007
13. D. C. Barber, B. H. Brown, "*Inverse problems in partial differential equations*", *Society for Industrial and Applied Mathematics Philadelphia*, 151-164, 1990
14. P. Metherall, R. H. Smallwood, D. C. Barber, "*Three dimensional electrical impedance tomography of the human thorax*", *Proceedings of the 18th Annual International Conference of the IEEE Engineering in Medicine and Biology Society*, 758 – 759, 1996
15. B. H. Brown, et al., "*Innovative Technology*". *Biol. Med.* Vol. 15, pp. 1-8, 1994
16. A. Borsic, C. McLeod, W. Lionheart and N. Lerrouche, "*Realistic 2D human thorax modelling for EIT*", *Journal of Physiological Measurement*, 22(1), 2001
17. N. Kerrouche, C. N. McLeod, W. R. B. Lionheart, "*Time series of EIT chest images using singular value decomposition and Fourier transform*", *Physiological Measurement*, 22(1): 147-157, 2001
18. W. Yan, S. Hong, Z. Shu, R. Chaoshi, "*Influences of compound electrode parameter on measurement sensitivity and reconstruction quality in electrical impedance tomography*", *Proceedings of International Federation for Medical and Biological Engineering*, 6, 2007
19. Uhlmann G., "*Developments in inverse problems since calderón's foundational paper, harmonic analysis and partial differential equations*", *Essays in Honor of Alberto P Calderón*, (editors ME Christ and CE Kenig), University of Chicago Press, 1999
20. B. H. Brown, D. C. Barber, and A. D. Seagar, "*Applied potential tomography: possible clinical applications*", *Clinical Physics and Physiological Measurement*, 6: 109-121, 1985.
21. A.V. Korjnevsky, "*Electrical impedance tomography: research, medical applications and commercialization*", *Troitsk Conference on Medical, Physics and Innovations in Medicine*", 2006
22. V. Cherepenin, A. Karpov, A. Korjnevsky, V. Kornienko, Y. Kultiasov, M. Ochapkin, O. Trochanova and D. Meister, "*Three-dimensional EIT imaging of breast tissues: system design and clinical testing*", *IEEE Transaction Medical Imaging*, 21(6): 662-667, 2002
23. V. Cherepenin, A. Karpov, A. Korjnevsky, V. Kornienko, A. Mazaletskaya, D Mazourov and D. Meister, "*A 3D electrical impedance tomography (EIT) system for breast cancer detection*", *Physiological Measurement*, 22(1): 9-18, 2001

24. G. A. Ybarra, Q. H. Liu, G. Ye, K. H. Lim, J. H. Lee, W. T. Joines, R. T. George, "*Breast imaging using electrical impedance tomography (EIT)*", Emerging Technology in Breast Imaging and Mammography, American Scientific Publishers, 2007
25. A. Hartov, N. K. Soni, K. D. Paulsen, "*Variation in breast EIT measurements due to menstrual cycle*", Physiological Measurement, 25: 295-299, 2004
26. O.V. Trokhanova, M.B. Okhapkin, A.V. Korjnevsky, V.N. Kornienko and V.A. Cherepenin "*Diagnostic possibilities of the electrical impedance mammography method*", Biomeditsinskaya Radioelektronika, 2: 66-77, 2009
27. Y F Mangnall et al, "*Comparison of applied potential tomography and impedance epigastrography as methods of measuring gastric emptying*", Physiological Measurement, 9: 249-254, 1987
28. B. M. Eyuboglu, B. H. Brown, D. C. Barber, "*In vivo imaging of cardiac related impedance changes*", IEEE Magazine Engineering in Medicine and Biology, 8(1): 39 – 45, 1989
29. H M Amasha, "*Quantitative assessment of impedance tomography for temperature measurements in microwave hyperthermia*", Clinical Physics and Physiological Measurement, 9: 49-53, 1987
30. S. Chaw, E. Yazaki, "*The effect of pH changes on the gastric emptying of liquid measured by electrical impedance tomography and pH-sensitive radio telemetry capsule C*" Department of Pharmaceutics, The School of Pharmacy, University of London, April 2001
31. T. P. Ryan, M. J. Moskowitz, K. D. Paulsen, "*The dartmouth electrical impedance tomography system For thermal imaging*", IEEE International Conference of Engineering in Medicine and Biology Society, 13(1): 321 – 322, 1991
32. K.R.Foster and H.P.Schwan, "*Dielectrical properties of tissues and biological materials: a critical review*", Critical Reviews in Biomedical Engineering, 17: 25-104, 1989
33. D.W.Davidson and R.H.Cole, "*Dielectric relaxation in glycerol, propylene glycol, and n-propanol*", Journal of Chem. Phys., 19: 1484-1490, 1951
34. X.Zhao, Y.Kinouchi, and E.Yasuno, "*A new method for non-invasive measurement of multilayer tissue conductivity and structure using divided electrode*", IEEE Transaction on Biomedical Engineering, 51(2): 362-370, 2004
35. X.Zhao, Y.Kinouchi, T.Iritani and et al., "*Estimation of multi-layer tissue conductivities from non-invasively measured bioresistances using divided electrodes*", IEICE Transactions on Information and Systems, E85-D(6):1031-1038, 2002
36. E. Tzanakou, R. Michalak, E. Harth "*The alopex process: visual receptive fields by response feedback*," Biol. Cybern., 35: 161-174, 1979
37. E. Harth, E. Tzanakou, "*Alopex, a stochastic method for determining visual receptive field*" Vision Research, 14: 1475-1482, 1974
38. E. Harth, K. P. Unnikrishnan, A. S. Pandya, "*The inversion of sensory processing by feedback pathways: A model of visual cognitive functions*", Science 237, pp. 184-187, 1987
39. A. S. Pandya, K. P. Venugopal, "*A stochastic parallel algorithm for supervised learning in neural networks*", IEICE Trans. on Information and Systems, E77-D(4): 376-384, 1994
40. A. S. Pandya, R. Szabo, "*Alopex algorithm for supervised learning in layered networks*", Proc. of International Neural Network Conference, Paris, 1990
41. K. P. Venugopal and A. S. Pandya, "*Alopex algorithm for training multilayer neural networks*", Proc. of International Joint Conference on Neural Networks, 1991
42. A. S. Pandya, R. B. Macy, "*Pattern Recognition with Neural Networks in C++*", CRC Press. Boca Raton and IEEE Press, 1995
43. P. S. Sastry, M. Magesh, K. P. Unnikrishnan, "*Two timescale analysis of the alopex algorithm for optimization*", Neural Computation, 14(11): 2729 – 2750, 2002
44. S Haykin, Z Chen, S Becker, "*Stochastic correlative learning algorithms*", IEEE Transactions on Signal Processing, 52(8): 2200 – 2209, 2004
45. A. Bia, "*Alopex-B: A new, simpler, but yet faster version of the alopex training algorithm*", International Journal of Neural Systems, 11(6): 497-507, 2001
46. Farzana Kabir Ahmad, Safaai Deris, Nor Hayati Othman, "*Toward integrated clinical and gene expression profiles for breast cancer prognosis: A review paper*", International Journal of Biometrics and Bioinformatics, 3(4): 31-47, 2009.

47. Ankur Agarwal, A. S. Pandya, Morrison S. Obeng, "A low power implementation of GMDH algorithm", Scientific International Journal of Computer Science, Informatics and Electrical Engineering, 2(1), 2008.
48. Shanthi Dhanushkodi, G.Sahoo , Saravanan Nallaperumal, "*Designing an artificial neural network model for the prediction of thrombo-embolic stroke*", International Journal of Biometrics and Bioinformatics, 3(1): 10-18, 2009